COMPDYN 2013
4th ECCOMAS Thematic Conference on
Computational Methods in Structural Dynamics and Earthquake Engineering
M. Papadrakakis, V. Papadopoulos, V. Plevris (eds.)
Kos Island, Greece, 12–14 June 2013

MULTI-SCALE ENERGY PUMPING BETWEEN A MAIN OSCILLATOR INCLUDING SAINT-VENANT TERM AND A NONLINEAR ENERGY SINK

M. Weiss[1], A. Ture Savadkoohi[2], and C.-H. Lamarque[2]

[1] Université de Lyon, École Nationale des Travaux Publics de l'État
LGCB
rue Maurice Audin, F-69518, Vaulx-en-Velin Cedex, France
e-mail: mathieu.weiss@entpe.fr

[2] Université de Lyon, École Nationale des Travaux Publics de l'État
LGCB and LTDS UMR CNRS 5513
rue Maurice Audin, F-69518, Vaulx-en-Velin Cedex, France
e-mail: {alireza.turesavadkoohi,lamarque}@entpe.fr

Keywords: Energy exchange, Saint-Venant, cubic, NES, nonlinear.

Abstract. *Vibratory energy exchange between oscillators can be used for localization, passive control and/or energy harvesting. It has been demonstrated, theoretically and experimentally, that by coupling an essential nonlinear and light oscillator to main oscillators, it will be possible to passively control the main system against externally induced forces. The phenomenon is called energy pumping and the nonlinear oscillator is named as nonlinear energy sink (NES). Some research works have been carried out in order to detect the energy pumping between linear and non-polynomial/nonsmooth NES systems or between a nonsmooth main oscillator and a coupled cubic NES. In this work, multi-scale vibratory energy exchange between a main oscillator including Saint-Venant term and a cubic nonlinear energy sink is studied. Analytically obtained invariant manifold of the system at fast time scale and detected fixed points and/or fold singularities at first slow time scale let us predict and explain different regimes that the system may face during the energy exchange process. The work will be accompanied by two numerical examples confirming our analytical developments.*

1 INTRODUCTION

It has been proved that by endowing nonlinear innate of some special light attachments, namely NES, it is possible to localize the energy of important oscillators which are mainely linear [1, 2, 3, 4, 5]. This localization can be for the aim of passive control and/or energy harvesting. The phenomenon is called energy pumping. The efficiency of NES systems in controlling main systems (e.g. in the field of acoustics, civil and mechanical engineering) has been proved experimentally as well [6, 7, 8, 9, 10, 11, 12]. Some works have been carried out in order to consider other types of nonlinearities for the NES: Nucera et al. [13], Lee et al. [14] and Gendelman [15] studied energy pumping in systems with vibro-impact NES. The energy pumping in a 2 dof system consisting of a linear dof and a nonlinear energy sink with non-polynomial and piece-wise potential investigated by Gendelman [16]. Lamarque et al. [17] pinpointed the targeted energy transfer phenomenon from a linear master dof system to a non-smooth NES under different forcing conditions while the same system in the presence of the gravity pinpointed by Ture Savadkoohi et al. [18]. Some researchers took into account the vibratory energy exchange between a non-smooth main oscillator and a coupled non-smooth/cubic NES: Schmidt and Lamarque [19] by endowing techniques of [20, 21] studied energy transfer from initial single dof system including non-smooth terms of friction type to a cubic NES. The behavior of two coupled non-smooth systems by detecting their invariant manifolds at different scales of time and finally their fixed point are enlightened in [22]. In this paper we would like to analytically investigate on the multi- scale energy exchange between two oscillators, namely a main one including Saint-Venant terms and a coupled cubic NES. Our analytical developments will be accompanied by two numerical examples. Organization of the paper is as it follows:
Academic model of the system, its re-scaling and averaging processes are given in Section 2. Time multi scale behavior of the system by detecting its invariant manifold and fixed points/fold singularities are described in Section 3. Comparison of analytical developments with obtained numerical results are illustrated in Section 4. Finally, conclusions are given in Section 5.

2 Mathematical presentation of the system

We consider a two dof system that is represented in Fig. 1. The main oscillator (M, k, $\tilde{\lambda}$) with a Saint-Venant type behavior ($\tilde{k}_p$, α) is coupled to a NES (m, $\tilde{C}_1$, $\tilde{\lambda}_1$) with cubic potential. The mass ratio between two oscillators is very small i.e., $0 < \epsilon = \dfrac{m}{M} \ll 1$

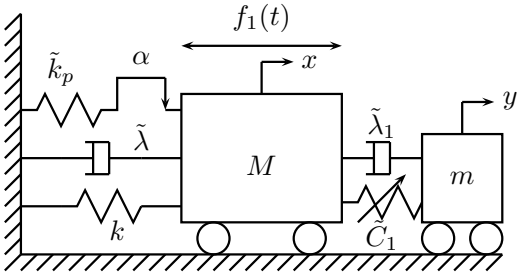

Figure 1: Academic model of the system

Governing equations of the described system in the Fig. 1 is summarized as:

$$\begin{cases} M\frac{d^2x}{dt^2} + \tilde{\lambda}\frac{dx}{dt} + \tilde{\lambda}_1(\frac{dx}{dt} - \frac{dy}{dt}) + kx + \tilde{k}_p u + \tilde{C}_1 F(x-y) = f_1(t) \\ m\frac{d^2y}{dt^2} + \tilde{\lambda}_1(\frac{dy}{dt} - \frac{dx}{dt}) + \tilde{C}_1 F(y-x) = 0 \\ \left(\frac{du}{dt} + \beta(\frac{\tilde{k}_p u}{\alpha})\right) \ni \frac{dx}{dt} \end{cases} \tag{1}$$

with $F : x \mapsto x^3$ and graph of β which is illustrated in Fig.2, is defined as:

$$\beta(x) = \begin{cases} \emptyset & \text{if} \quad x \in]-\infty, -1[\cup]1, +\infty[\\ 0 & \text{if} \quad x \in]-1, 1[\\ \mathbb{R}_- & \text{if} \quad x = -1 \\ \mathbb{R}_+ & \text{if} \quad x = 1 \end{cases} \tag{2}$$

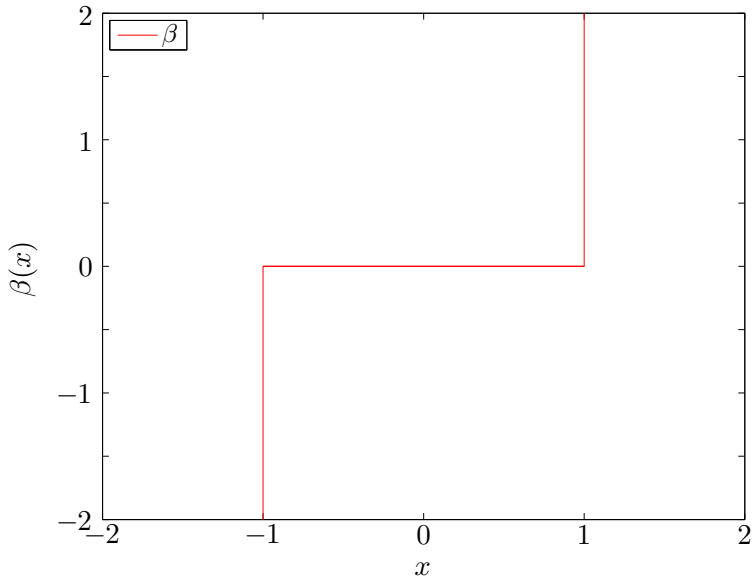

Figure 2: Graph of β

Let us suppose that $\tau = t\sqrt{\frac{k}{M}} = w_1 t$. We introduce following variables: $\frac{\tilde{\lambda} w_1}{M w_1^2} = \epsilon\lambda_0$, $\frac{\tilde{k}_p}{M w_1^2} = \epsilon k_p$, $\frac{\tilde{C}_1}{M w_1^2} = \epsilon C_{10}$, $\frac{\tilde{\lambda}_1}{M w_1^2} = \epsilon\lambda_{10}$, $\frac{f_1(\frac{\tau}{\omega_1})}{M w_1^2} = \epsilon f_{10}\sin(\Omega\tau)$, $\eta = \frac{\alpha}{\tilde{k}_p}$. The system (1) reads (for any arbitrary function V, $\frac{dV}{d\tau}$ is denoted by V'):

$$\begin{cases} x'' + \epsilon\lambda_0 x' + \epsilon\lambda_{10}(x' - y') + x + \epsilon k_p u + \epsilon C_{10} F(x-y) = \epsilon f_{10}\sin(\Omega\tau) \\ \epsilon y'' + \epsilon\lambda_{10}(y' - x') + \epsilon C_{10} F(y-x) = 0 \\ \left(u' + \beta(\frac{u}{\eta})\right) \ni x' \end{cases} \tag{3}$$

Coordinates of the center of mass and relative displacement of two masses are introduced as:

$$\left\{\begin{array}{lcl} v &=& x+\epsilon y \\ w &=& x-y \end{array}\right. \Leftrightarrow \left\{\begin{array}{lcl} x &=& \frac{v+\epsilon w}{1+\epsilon} \\ y &=& \frac{v-w}{1-\epsilon} \end{array}\right. \tag{4}$$

System (3) in new coordinates is defined as:

$$\left\{\begin{array}{l} v''+\epsilon\lambda_0\frac{v'+\epsilon w'}{1+\epsilon}+\frac{v+\epsilon w}{1+\epsilon}+\epsilon k_p u=\epsilon f_{10}\sin(\Omega\tau) \\ w''+\epsilon\lambda_0\frac{v'+\epsilon w'}{1+\epsilon}+\frac{v+\epsilon w}{1+\epsilon}+\epsilon k_p u+(1+\epsilon)(\lambda_{10}w'+C_{10}F(w))=\epsilon f_{10}\sin(\Omega\tau) \\ \left(u'+\beta(\frac{u}{\eta})\right)\ni\frac{v'+\epsilon w'}{1+\epsilon} \end{array}\right. \tag{5}$$

We assume that $\tilde{\tau}=\Omega\tau$ and then following complex variables of Manevitch [23] are introduced to the system (5)(for any arbitrary function V, $\frac{dV}{d\tilde{\tau}}$ is denoted by $\dot{V}$):

$$\left\{\begin{array}{lcl} \phi_1 e^{i\tilde{\tau}} &=& \Omega(\dot{v}+iv) \\ \phi_2 e^{i\tilde{\tau}} &=& \Omega(\dot{w}+iw) \\ \phi_3 e^{i\tilde{\tau}} &=& \Omega(\dot{u}+iu) \end{array}\right. \tag{6}$$

We endow the Galerkin method using truncated Fourier series. In this paper we consider only first harmonic, i.e. $e^{i\tilde{\tau}}$, for each equation. Based on the general periodic behavior of system variables we obtain (see for example [18]):

$$\left\{\begin{array}{l} \Omega\dot{\phi_1}-\frac{\Omega}{2i}\phi_1+\frac{\epsilon\lambda_0(\phi_1+\epsilon\phi_2)}{2(1+\epsilon)}+\frac{\phi_1+\epsilon\phi_2}{2i\Omega(1+\epsilon)}+\frac{\epsilon k_p}{2\Omega i}\phi_3=\epsilon\frac{f_{10}}{2i} \\ \Omega\dot{\phi_2}-\frac{\Omega}{2i}\phi_2+\frac{\epsilon\lambda_0(\phi_1+\epsilon\phi_2)}{2(1+\epsilon)}+\frac{\phi_1+\epsilon\phi_2}{2i\Omega(1+\epsilon)}+\frac{\epsilon k_p}{2\Omega i}\phi_3 \\ +(1+\epsilon)(C_{10}\mathcal{F}+\frac{\lambda_{10}}{2}\phi_2)=\epsilon\frac{f_{10}}{2i} \\ \phi_3=\frac{\phi_1+\epsilon\phi_2}{(1+\epsilon)\pi}\xi\left(\frac{|\phi_1+\epsilon\phi_2|}{(1+\epsilon)\Omega}\right) \end{array}\right. \tag{7}$$

where

$$\forall z\in\mathbb{R}_+,\xi(z)=\left\{\begin{array}{ll} \pi & if\ \ z\leqslant\eta \\ \bar{\tau}_1+e^{-i\bar{\tau}_1}\sin(\bar{\tau}_1)-4e^{-i\frac{\bar{\tau}_1}{2}}\sin(\frac{\bar{\tau}_1}{2})-\frac{4\eta}{z}e^{-i(\bar{\tau}_1+\frac{\pi}{2})} & if\ \ z>\eta \end{array}\right. \tag{8}$$

and

$$\bar{\tau}_1=\arccos(1-\frac{2\eta}{z}) \tag{9}$$

The averaging process (i.e. truncated Fourier series and keeping first harmonic) of the third equation of the system (5) is described in appendix A. We will analyze system behavior around $1:1$ resonance, i.e. $\Omega=1+\epsilon\sigma$.

3 Multi-scale analysis of the system

An asymptotic approach [24] is used by introducing fast time $\tilde{\tau}_0$ and slow times $\tilde{\tau}_1$, $\tilde{\tau}_2$...

$$\tilde{\tau} = \tilde{\tau}_0, \tilde{\tau}_1 = \epsilon\tilde{\tau}_0, ... \tag{10}$$

so

$$\frac{d}{d\tilde{\tau}} = \frac{\partial}{\partial\tilde{\tau}_0} + \epsilon\frac{\partial}{\partial\tilde{\tau}_1} + ... \tag{11}$$

We study the system at different orders of ϵ.

3.1 ϵ^0 order

At the ϵ^0 order, following equations can be derived from the system (7):

$$\frac{\partial\phi_1}{\partial\tilde{\tau}_0} = 0 \Rightarrow \phi_1 = \phi_1(\tilde{\tau}_1) \tag{12}$$

$$\frac{\partial\phi_2}{\partial\tilde{\tau}_0} - \frac{\phi_2}{2i} + \frac{\phi_1}{2i} + C_{10}\mathcal{F} + \frac{\lambda_{10}}{2}\phi_2 = 0 \tag{13}$$

$$\phi_3 = \frac{\phi_1}{\pi}\xi(|\phi_1|) \tag{14}$$

Since we are dealing with cubic nonlinearity of the NES, i.e. $F : x \mapsto x^3$, then it is possible to obtain its average, $\mathcal{F}$, as a function of ϕ_2:

$$\mathcal{F} = \frac{1}{2i}G(|\phi_2|^2)\phi_2 \;\; with \;\; G : x \mapsto \frac{3x}{4} \tag{15}$$

Fixed points, which corresponding to the behavior of ϕ_2 for $\tilde{\tau}_0 \to +\infty$, can be obtained from equation (13):

$$\phi_1 = \phi_2 - C_{10}G(|\phi_2|^2)\phi_2 - i\lambda_{10}\phi_2 \tag{16}$$

If we suppose that $\phi_1 = N_1e^{i\delta_1}$ and $\phi_2 = N_2e^{i\delta_2}$ ($N_1 \in \mathbb{R}_+$,$N_2 \in \mathbb{R}_+$, $\delta_1 \in \mathbb{R}$ and $\delta_2 \in \mathbb{R}$), then equation (16) reads:

$$N_1 = N_2\sqrt{(1 - C_{10}G(N_2^2))^2 + \lambda_{10}^2} \tag{17}$$

$$\begin{cases} \Delta\delta = \delta_2 - \delta_1 = \arctan\left(\frac{\lambda_{10}}{1-C_{10}G(N_2^2)}\right) & \text{if} \quad 1 - C_{10}G(N_2^2) > 0 \\ \Delta\delta = \delta_2 - \delta_1 = \arctan\left(\frac{\lambda_{10}}{1-C_{10}G(N_2^2)}\right) + \pi & \text{if} \quad 1 - C_{10}G(N_2^2) < 0 \end{cases} \tag{18}$$

Equation (17) gives the invariant manifold of the system at fast time scale. Figure 3 represents this invariant for some given system parameters. Now, we would like to seek for local extrema of the Eq. (17). We have:

$$\frac{\partial N_1^2}{\partial N_2^2} = ((1 - C_{10}G(N_2^2))^2 + \lambda_{10}^2) - 2C_{10}N_2^2G'(N_2^2) + 2N_2^2G'(N_2^2)G(N_2^2) = 0 \tag{19}$$

so according to (15)

$$\frac{\partial N_1^2}{\partial N_2^2} = \frac{27}{16}C_{10}^2N_2^4 - 3C_{10}N_2^2 + \lambda_{10}^2 + 1 = 0 \tag{20}$$

$$\Delta = 9 - 4\frac{27}{16}(1+\lambda_{10}^2) \tag{21}$$

and

$$\Delta \geqslant 0 \Leftrightarrow \lambda_{10} \leqslant \frac{1}{\sqrt{3}} \tag{22}$$

Coordinates of local extrema (N_{2+}, N_{1+}) and (N_{2-}, N_{1-}), are summarized as:

$$N_{2+} = \sqrt{\frac{24+8\sqrt{\Delta}}{27C_{10}}} \quad so \quad N_{1+} = N_{2+}\sqrt{(1-C_{10}G(N_{2+}^2))^2+\lambda_{10}^2} \tag{23}$$

$$N_{2-} = \sqrt{\frac{24-8\sqrt{\Delta}}{27C_{10}}} \quad so \quad N_{1-} = N_{2-}\sqrt{(1-C_{10}G(N_{2-}^2))^2+\lambda_{10}^2} \tag{24}$$

These coordinates are shown in Fig. 3. Stability borders of the invariant manifold which are

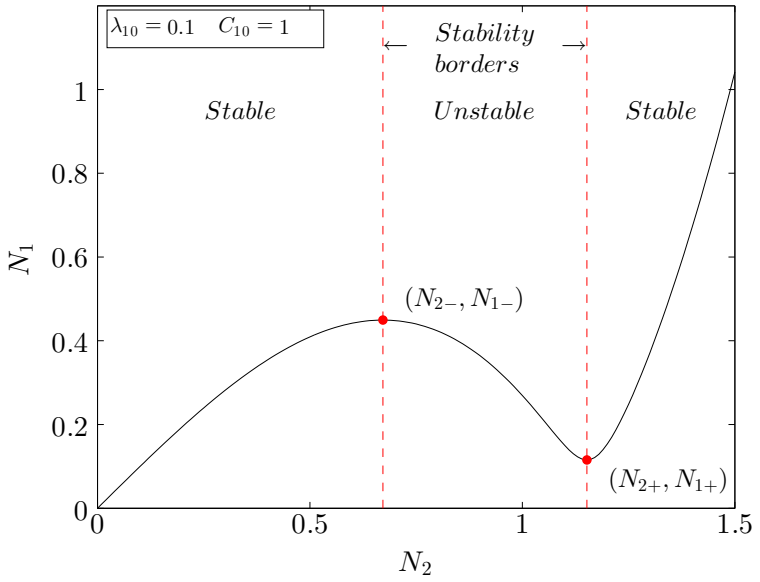

Figure 3: Invariant manifold of the system and its stability borders.

represented in Figure 3 can be detected by perturbing N_2 and δ_2 in system (13) as $N_2 + \Delta N_2$ and $\delta_2 + \Delta\delta_2$ [17, 18].

3.2 ϵ^1 order

The ϵ^1 order of first equation of system (7) gives:

$$\frac{\partial\phi_1}{\partial\tilde{\tau_1}} + \frac{\lambda_0}{2}\phi_1 + \frac{\phi_2}{2i} - \frac{2\sigma+1}{2i}\phi_1 + \frac{k_p}{2i}\phi_3 = \frac{f_{10}}{2i} \tag{25}$$

From this moment on for respecting ϵ^1 order of system of equations, evolution of ϕ_3 at ϵ^0 order which is defined in (14) should be considered in Eq. (25) and all relevant forthcoming analytical developments. If $N_1 > \eta$, ϕ_3 reads:

$$\begin{aligned} \phi_3 &= \tfrac{\phi_1}{\pi}[\bar{\tau_1} + e^{-i\bar{\tau_1}}\sin(\bar{\tau_1}) - 4e^{-i\frac{\bar{\tau_1}}{2}}\sin(\tfrac{\bar{\tau_1}}{2}) - \tfrac{4\eta}{|\phi_1|}e^{-i(\bar{\tau_1}+\frac{\pi}{2})}] \\ &= [\tilde{\mathcal{F}}_{re}(N_1) + i\tilde{\mathcal{F}}_{im}(N_1)]e^{i\delta_1} \end{aligned} \tag{26}$$

where

$$\begin{aligned}\tilde{\mathcal{F}}_{re}(N_1) &= \frac{N_1}{\pi}[\bar{\tau_1} + \sin(\bar{\tau_1})\cos(\bar{\tau_1}) - 4\cos(\frac{\bar{\tau_1}}{2})\sin(\frac{\bar{\tau_1}}{2}) + \frac{4\eta}{N_1}\sin(\bar{\tau_1})] \\ \tilde{\mathcal{F}}_{im}(N_1) &= \frac{N_1}{\pi}[-\sin^2(\bar{\tau_1}) + 4\sin^2(\frac{\bar{\tau_1}}{2}) + \frac{4\eta}{N_1}\cos(\bar{\tau_1})]\end{aligned} \tag{27}$$

If $N_1 \leqslant \eta$, we have the same notations with $\tilde{\mathcal{F}}_{re}(N_1) = N_1$ and $\tilde{\mathcal{F}}_{im}(N_1) = 0$. Considering equation (17), ϕ_3 can be obtained as a function of N_2 and δ_1 with new definitions $\mathcal{F}_{re}$ and $\mathcal{F}_{im}$ which are derived from $\tilde{\mathcal{F}}_{re}$ and $\tilde{\mathcal{F}}_{im}$:

$$\phi_3 = [\mathcal{F}_{re}(N_2) + i\mathcal{F}_{im}(N_2)]e^{i\delta_1} \tag{28}$$

From equation (16) we have:

$$\begin{aligned}\frac{\partial\phi_1}{\partial\tilde{\tau_1}} &= -2\frac{\partial N_2}{\partial\tilde{\tau_1}}N_2C_{10}G'(N_2^2)e^{i\delta_2} + (1 - C_{10}G(N_2^2) - i\lambda_{10})(\frac{\partial N_2}{\partial\tilde{\tau_1}}e^{i\delta_2} + iN_2\frac{\partial\delta_2}{\partial\tilde{\tau_1}}e^{i\delta_2}) \\ &= \frac{f_0}{2i} - \frac{\lambda_0}{2}(1 - C_{10}G(N_2^2) - i\lambda_{10})N_2e^{i\delta_2} - \frac{1}{2i}N_2e^{i\delta_2} \\ &\quad + \frac{2\sigma+1}{2i}(1 - C_{10}G(N_2^2) - i\lambda_{10})N_2e^{i\delta_2} \\ &\quad - \frac{k_p}{2i}(\mathcal{F}_{re}(N_2) + i\mathcal{F}_{im}(N_2))e^{\delta_1}\end{aligned} \tag{29}$$

After separating real and imaginary parts

$$\begin{cases} -2C_{10}N_2^2G'(N_2^2)\frac{\partial N_2}{\partial\tilde{\tau_1}} + \lambda_{10}N_2\frac{\partial\delta_2}{\partial\tilde{\tau_1}} + (1 - C_{10}G(N_2^2))\frac{\partial N_2}{\partial\tilde{\tau_1}} &= \Xi(N_2,\delta_2) \\ (1 - C_{10}G(N_2^2))N_2\frac{\partial\delta_2}{\partial\tilde{\tau_1}} - \lambda_{10}\frac{\partial N_2}{\partial\tilde{\tau_1}} &= \Sigma(N_2,\delta_2) \end{cases} \tag{30}$$

with

$$\begin{aligned}\Xi(N_2,\delta_2) &= -\frac{f_0}{2}\sin(\delta_2) - \frac{(2\sigma+1)\lambda_{10}}{2}N_2 - \frac{\lambda_0}{2}(1 - C_{10}G(N_2^2))N_2 \\ &\quad - \frac{k_p}{2}(\mathcal{F}_{im}(N_2)\cos(\Delta\delta) - \mathcal{F}_{re}(N_2)\sin(\Delta\delta)) \\ \Sigma(N_2,\delta_2) &= -\frac{f_0}{2}\cos(\delta_2) - \frac{2\sigma+1}{2}(1 - C_{10}G(N_2^2))N_2 + \frac{\lambda_0\lambda_{10}}{2}N_2 + \frac{N_2}{2} \\ &\quad + \frac{k_p}{2}(\mathcal{F}_{im}(N_2)\sin(\Delta\delta) + \mathcal{F}_{re}(N_2)\cos(\Delta\delta))\end{aligned} \tag{31}$$

The function C is introduced as:

$$C(N_2) = \lambda_{10}^2 - 2C_{10}N_2^2G'(N_2^2)(1 - C_{10}G(N_2^2)) + (1 - C_{10}G(N_2^2))^2 \tag{32}$$

Then system (30) reads:

$$\begin{cases} C(N_2)\frac{\partial N_2}{\partial\tilde{\tau_1}} &= (1 - C_{10}G(N_2^2))\Xi(N_2,\delta_2) - \lambda_{10}\Sigma(N_2,\delta_2) \\ C(N_2)N_2\frac{\partial\delta_2}{\partial\tilde{\tau_1}} &= \lambda_{10}\Xi(N_2,\delta_2) + (1 - C_{10}G(N_2^2) - 2C_{10}N_2^2G'(N_2^2))\Sigma(N_2,\delta_2) \end{cases} \tag{33}$$

This can be re-written in a compact form as:

$$\begin{cases} \frac{\partial N_2}{\partial\tilde{\tau_1}} &= \frac{f(N_2,\delta_2)}{C(N_2)} \\ \frac{\partial\delta_2}{\partial\tilde{\tau_1}} &= \frac{g(N_2,\delta_2)}{N_2C(N_2)} \end{cases} \tag{34}$$

Functions f and g are given in appendix B. By studying zeros of functions f, g and C in the reduced system (34), one can detect fixed points ($f = g = 0$ and $C \neq 0$) which correspond to periodic regimes and fold singularities ($f = g = C = 0$) which are signs of strongly modulated responses of the system.

4 Numerical examples

The exact behavior of the system will be compared with analytical predictions. The exact response of the system is obtained by numerically integration of the system (3) and then by using explained change of variables in (4) and (6). Analytical predictions will be obtained by using equations (17) as analytical invariant manifold and the system (34) for obtaining fixed points and fold singularities. System (3) is integrated during 100000 unit of time τ with time steps equal to $\Delta\tau = 10^{-5}$ by using an Euler numerical scheme explained in [19]. This scheme is convergent with order 1. Parameters are $C_{10} = 1$, $\lambda_{10} = 0.1$ (as in Figure 3) $\lambda_0 = 0.1$, $\eta = 0.3$, $k_p = 1$ and $\epsilon = 0.001$. Assumed initial conditions are $x(0) = 0.5$, $u(0) = 0.3$, and zero for other coordinates. These initial conditions are illustrated with $\times$ symbol in all relevant figures.

4.1 Example 1: $f_{10} = 0.3$

All possible areas where functions $f(N_2, \delta_2)$, $g(N_2, \delta_2)$ and $C(N_2)$ in Eq. (34) become zero are presented in Figure 4. It can be seen that the system possesses one fixed points and two fold singularities on the lower fold line. Phase portraits of the system around its fixed point is depicted in Figure 5 showing that this fixed point which corresponds to a periodic regime is stable. Analytical invariant manifold of the system which is obtained by Eq. (17) and corresponding numerical ones are illustrated in Figure 6. This shows that the averaged behavior of the system follows its invariant manifold and when it reaches to the stability border, it experiences a bifurcation by a jump to other stable branch. Finally the system is attracted by its fixed point (Point A in Figure 6) which corresponds to a periodic regime. This behavior can be seen more clearly in the time domain by looking histories of system amplitudes that are illustrated in Figures 7 and 8. These histories show that the system after experiencing a bifurcation, which corresponds to sudden energy loss of the NES and almost constat energy level for the main system, finally is attracted to a periodic regime which corresponds to the fixed point A.

4.2 Example 2: $f_{10} = 1$

All possible dynamics of the system are collected in Figure 9. Here, the system possesses one fixed point, A $(5.97, 1.05)$, and two fold singularities, α $(3.66, 0.67)$ and β $(6.06, 0.67)$. Overall view of the phase portrait of the system which is given in Figure 10 shows that α and β are in the form of node and saddle fold singularities. Existence of these fold singularities which are detected by developed analytical techniques give us a hint of possible existence of strongly modulated response (SMR) [17, 25]. Analytical invariant manifold of the system and corresponding numerical results are illustrated in Figure 11 showing that real behavior of the system follows its invariant manifold. This figure highlights the persistent SMR of the system by hysterically jumps between its fold lines (are obtained by setting $C(N_2) = 0$). Variations of system amplitudes which are depicted in Figure 12 and Figure 13 shows that two oscillators present beating response during the SMR. This kind of behavior is very interesting for passive control and/or energy harvesting by proper design of the NES in such a way that the difference

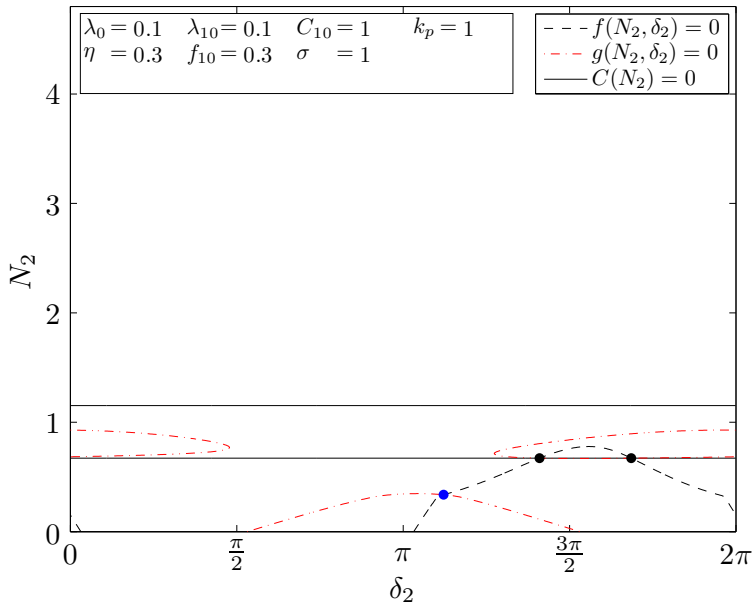

Figure 4: Dynamics of the system under forcing term $f_{10} = 0.3$: positions of fixed point and fold singularities.

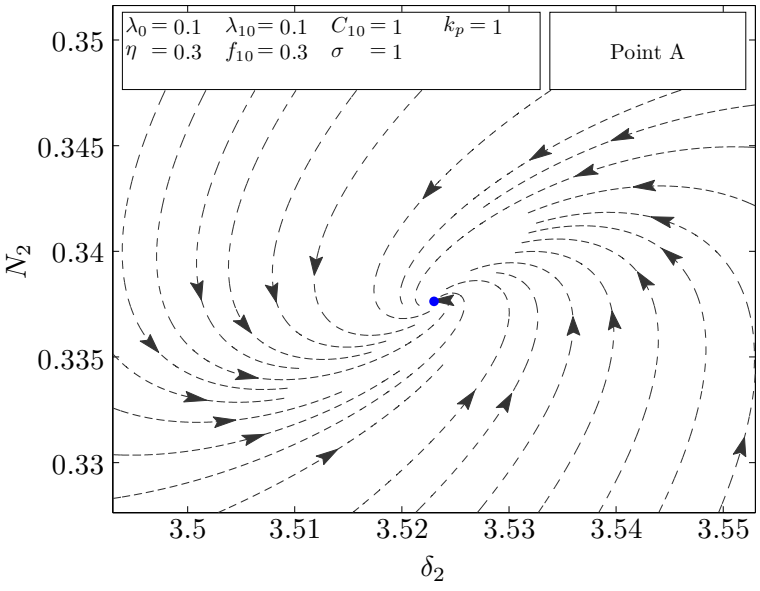

Figure 5: Phase portrait of the system under external forcing term $f_{10} = 0.3$ around its fixed point.

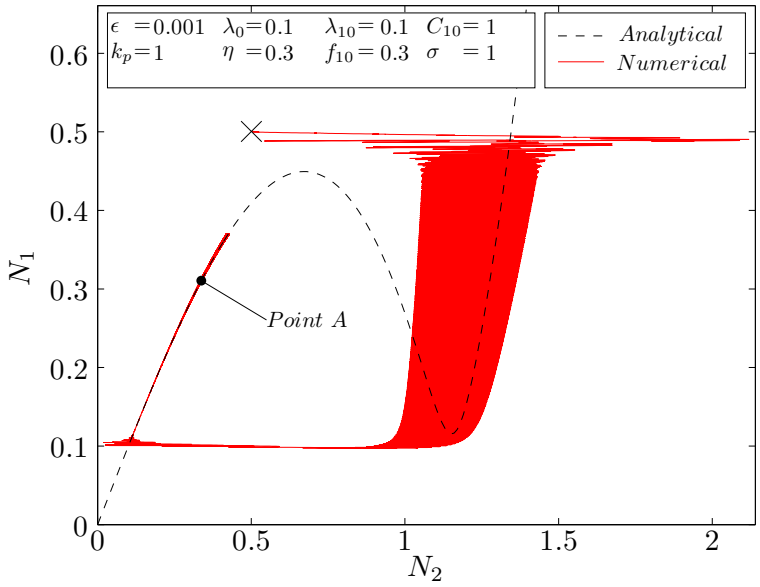

Figure 6: Invariant manifold of the system and corresponding numerical results under forcing term $f_{10} = 0.3$: initial conditions are shown by $\times$ symbol.

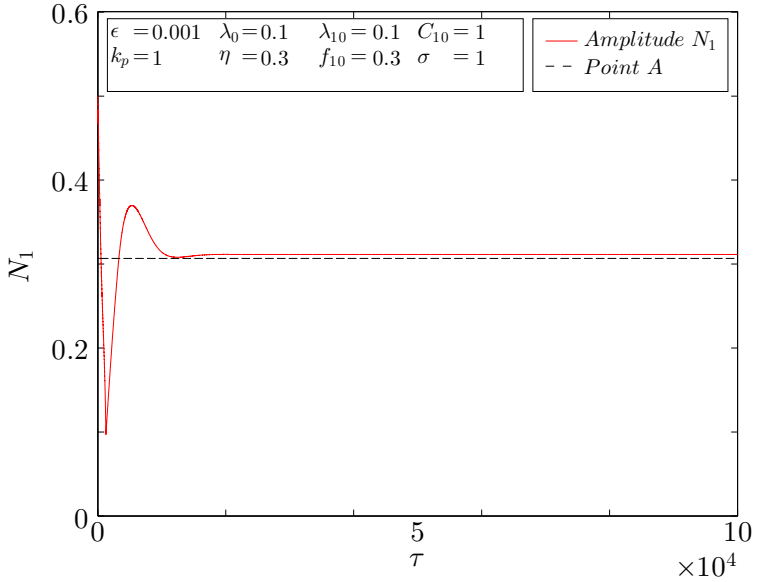

Figure 7: History the N_1 versus time τ for the system under forcing term $f_{10} = 0.3$.

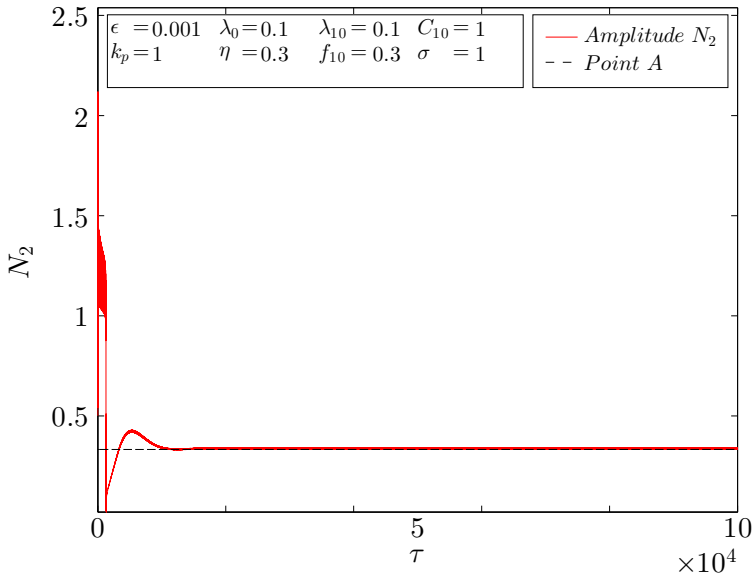

Figure 8: History the N_2 versus time τ for the system under forcing term $f_{10} = 0.3$.

between local maximum and minimum of the invariant, namely N_{1-} and N_{1+}, be small while the same difference in the N_2 direction, i.e. between N_{2-} and N_{2+}, can be large. In this case a high amounts of energy are trapped in a cycle which can be used for harvesting as well.

It is worthwhile to mention that obtained numerical results automatically contain all harmonics of the system while the analytical invariant manifold is based on keeping just first harmonics and truncating higher ones. This is the reason of oscillations of numerical results around the analytical invariant manifold which also causes the start of the bifurcation not to be exactly from the local minimum of the theoretical invariant manifold.

5 Conclusion

We presented the behavior of a two dof nonlinear system. In detail: the main dof includes Saint-Venant terms and the other coupled dof is a nonlinear energy sink with cubic potential. Analytically detected invariant manifold at the fast time scale let us predict the flow of system amplitudes while traced system behavior at first slow time scale let us collect its fixed points and fold singularities. According to external forcing terms (for given initial conditions) the system may face periodic and/or strongly modulated responses. These regimes can represent low or hight energy levels and/or persistently energy exchange between two oscillators by hysteresis bifurcations. Developed techniques in this paper can be used for designing nonlinear energy sink devices for the aim of localization which can be passive control, energy harvesting or both of them.

Acknowledgment

Authors would like to thank the "Ministère de l'Écologie, du Développement Durable et de l'Énergie" for supporting this research.

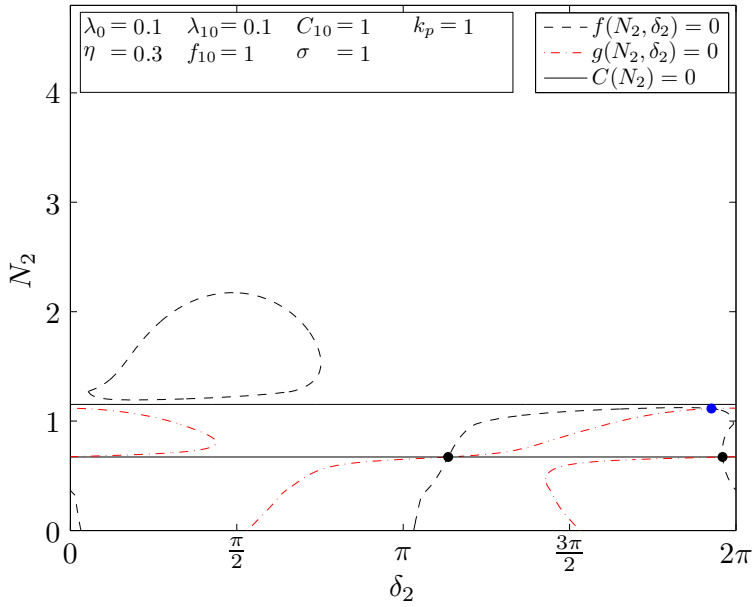

Figure 9: Dynamics of the system under forcing term $f_{10} = 1$: positions of fixed point and fold singularities.

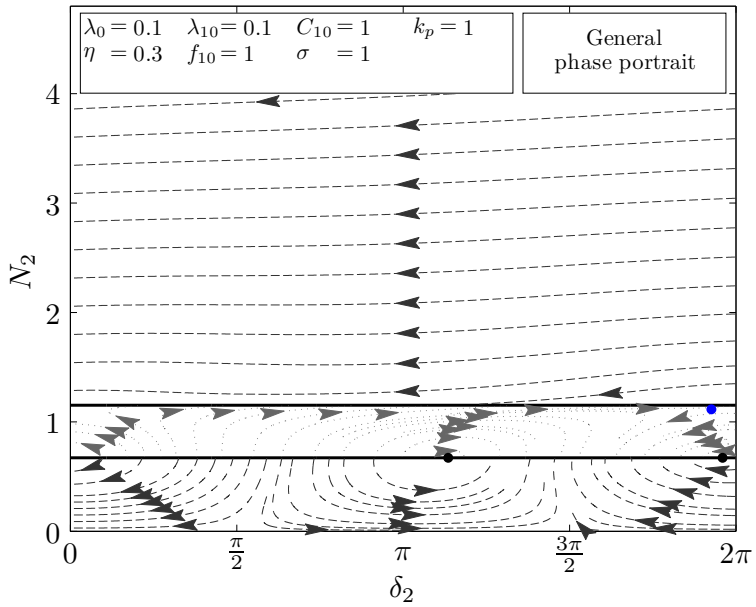

Figure 10: Dynamics of the system under forcing term $f_{10} = 1$: overall view of the phase portrait.

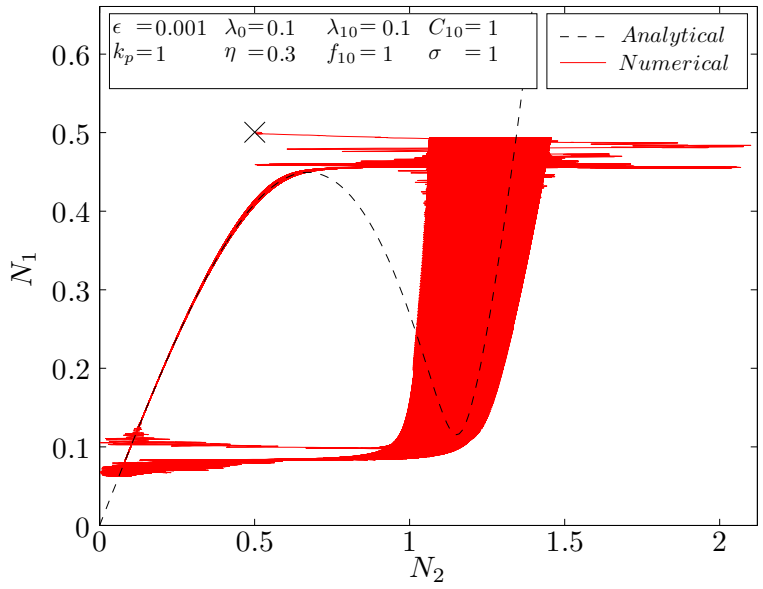

Figure 11: Invariant manifold of the system and corresponding numerical results under forcing term $f_{10} = 1$: initial conditions are shown by $\times$ symbol.

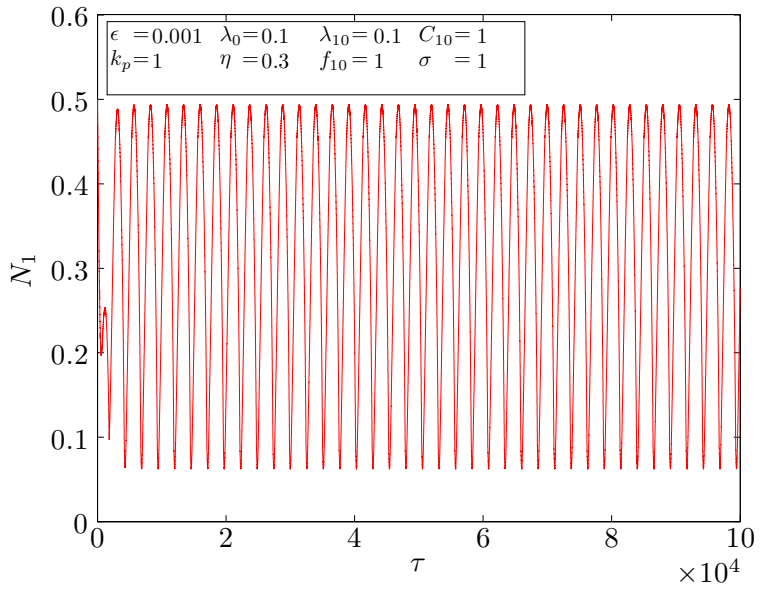

Figure 12: History the N_1 versus time τ for the system under forcing term $f_{10} = 1$.

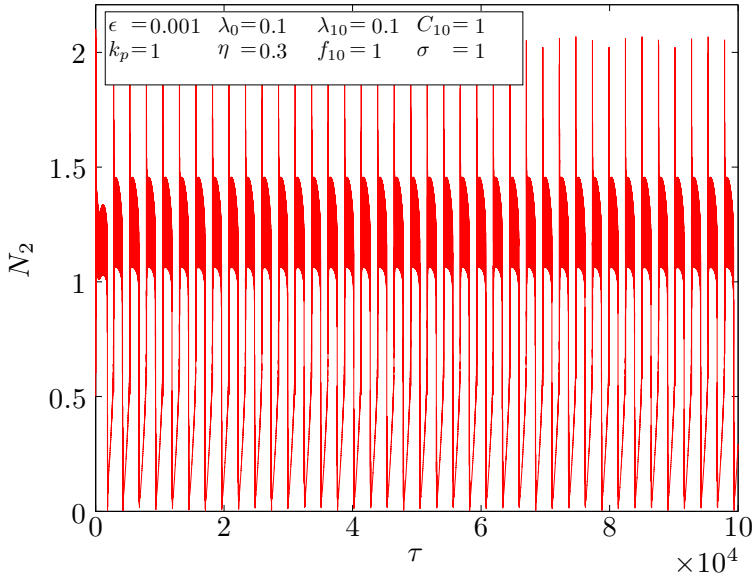

Figure 13: History the N_2 versus time τ for the system under forcing term $f_{10} = 1$.

Appendix

A Averaging ϕ_3

Here, we implement the Galerkin method by using a truncated Fourier series and keeping first harmonic, i.e. $e^{i\tilde{\tau}}$.

ϕ_3 is in relation with the u. u depends on the displacement x, which can be written as (35):

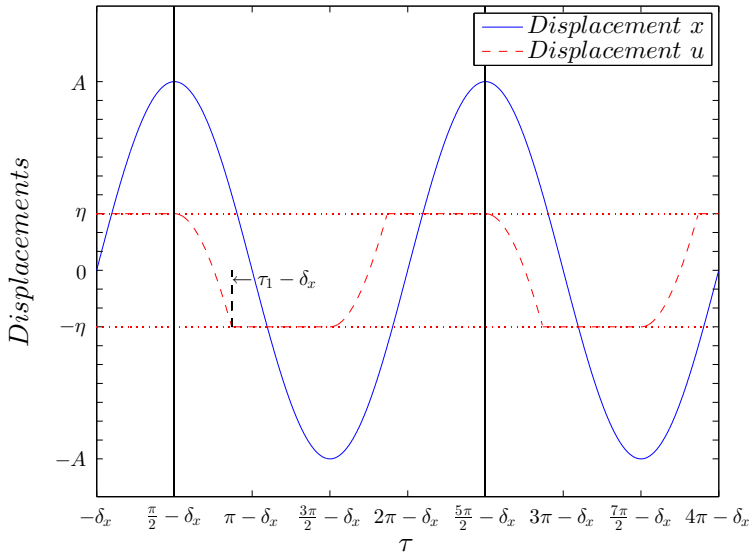

Figure 14: Displacements x and u

$$x(\tilde{\tau}) = A_x \sin(\tilde{\tau} + \delta_x) \tag{35}$$

where:

$$\Omega A_x = \frac{|\phi_1 + \epsilon\phi_2|}{1+\epsilon} \ \ and \ \ \delta_x = Arg\Big(\frac{\phi_1 + \epsilon\phi_2}{1+\epsilon}\Big) \tag{36}$$

If A_x is smaller than η, Saint-Venant element is only a stiffness, $x = u$, so:

$$\phi_3 = \frac{\phi_1 + \epsilon\phi_2}{1+\epsilon} \tag{37}$$

If $A_x > \eta$, the general qualitative behavior of u is presented in Fig. 14. On the interval of $[\frac{\pi}{2} - \delta_x; \frac{5\pi}{2} - \delta_x]$ we have:

$$A_x \cos(\tau_1 - \frac{\pi}{2}) = A_x - 2\eta \ \ so \ \ \tau_1 = \arccos(1 - \frac{2\eta}{A_x}) + \frac{\pi}{2} \tag{38}$$

then,

$$\begin{aligned}
\tfrac{\phi_3}{2i\Omega} &= \tfrac{1}{2\pi}\textstyle\int_{\frac{\pi}{2}-\delta_x}^{\frac{5\pi}{2}-\delta_x} e^{-i\tilde{\tau}}u(\tilde{\tau})d\tilde{\tau} = \tfrac{e^{i\delta_x}}{2\pi}\textstyle\int_{\frac{\pi}{2}}^{\frac{5\pi}{2}} e^{-i\tilde{\tau}}u(\tilde{\tau}-\delta_x)d\tilde{\tau} \\
&= \tfrac{e^{i\delta_x}}{2\pi}\Big[\textstyle\int_{\frac{\pi}{2}}^{\tau_1} e^{-i\tilde{\tau}}[x(\tilde{\tau}-\delta_x) - (A_x-\eta)]d\tilde{\tau} + \int_{\tau_1}^{\frac{3\pi}{2}} e^{-i\tilde{\tau}}(-\eta)d\tilde{\tau} \\
&\quad + \textstyle\int_{\frac{3\pi}{2}}^{\tau_1+\pi} e^{-i\tilde{\tau}}[x(\tilde{\tau}-\delta_x) + (A_x-\eta)]d\tilde{\tau} + \int_{\tau_1+\pi}^{\frac{5\pi}{2}} e^{-i\tilde{\tau}}\eta d\tilde{\tau}\Big] \\
&= \tfrac{e^{i\delta_x}}{\pi}\Big[\textstyle\int_{\frac{\pi}{2}}^{\tau_1} e^{-i\tilde{\tau}}x(\tilde{\tau}-\delta_x)d\tilde{\tau} - \int_{\frac{\pi}{2}}^{\tau_1} e^{-i\tilde{\tau}}(A_x-\eta)d\tilde{\tau} - \int_{\tau_1}^{\frac{3\pi}{2}} e^{-i\tilde{\tau}}\eta d\tilde{\tau}\Big] \\
&= \tfrac{e^{i\delta_x}}{\pi}\Big[\textstyle\int_{\frac{\pi}{2}}^{\tau_1} e^{-i\tilde{\tau}}x(\tilde{\tau}-\delta_x)d\tilde{\tau} - i(A_x-\eta)(e^{-i\tau_1}+i) - i\eta(i-e^{-i\tau_1})\Big] \\
&= \tfrac{e^{i\delta_x}}{\pi}\Big[\textstyle\int_{\frac{\pi}{2}}^{\tau_1} e^{-i\tilde{\tau}}x(\tilde{\tau}-\delta_x)d\tilde{\tau} - iA_x(e^{-i\tau_1}+i) + 2i\eta e^{-i\tau_1}\Big] \\
&= \tfrac{e^{i\delta_x}}{\pi}\Big[\tfrac{A_x}{2i}[(\tau_1 - \tfrac{\pi}{2}) - \tfrac{i}{2}(e^{-2i\tau_1}+1)] - iA_x(e^{-i\tau_1}+i) + 2i\eta e^{-i\tau_1}\Big] \\
&= \tfrac{A_x e^{i\delta_x}}{2\pi i}\Big[(\tau_1 - \tfrac{\pi}{2}) + e^{-i(\tau_1+\frac{\pi}{2})}\cos(\tau_1) + 4e^{\frac{i}{2}(\frac{\pi}{2}-\tau_1)}\cos(\tfrac{\tau_1}{2}+\tfrac{\pi}{4}) - \tfrac{4\eta}{A_x}e^{-i\tau_1}\Big]
\end{aligned} \tag{39}$$

with $\bar{\tau_1} = \tau_1 - \frac{\pi}{2}$, we have:

$$\phi_3 = \frac{\phi_1 + \epsilon\phi_2}{(1+\epsilon)\pi}\Big[\bar{\tau_1} + e^{-i\bar{\tau_1}}\sin(\bar{\tau_1}) - 4e^{-i\frac{\bar{\tau_1}}{2}}\sin(\frac{\bar{\tau_1}}{2}) - \frac{4\eta\Omega(1+\epsilon)}{|\phi_1+\epsilon\phi_2|}e^{-i(\bar{\tau_1}+\frac{\pi}{2})}\Big] \tag{40}$$

so with function ξ as notation with $\bar{\tau_1} = \arccos(1 - \frac{2\eta}{A_x})$:

$$\xi(A_x) = \begin{cases} \pi & if \ \ A_x \leqslant \eta \\ \bar{\tau_1} + e^{-i\bar{\tau_1}}\sin(\bar{\tau_1}) - 4e^{-i\frac{\bar{\tau_1}}{2}}\sin(\frac{\bar{\tau_1}}{2}) - \frac{4\eta}{A_x}e^{-i(\bar{\tau_1}+\frac{\pi}{2})} & if \ \ A_x > \eta \end{cases} \tag{41}$$

Final written of ϕ_3 for all values is:

$$\phi_3 = \frac{\phi_1 + \epsilon\phi_2}{(1+\epsilon)\pi}\xi(\frac{|\phi_1+\epsilon\phi_2|}{(1+\epsilon)\Omega}) \tag{42}$$

B Functions f and g

$$
\begin{aligned}
f(N_2,\delta_2) &= (1-C_{10}G(N_2^2))(-\tfrac{f_0}{2}\sin(\delta_2)-\tfrac{(2\sigma+1)\lambda_{10}}{2}N_2-\tfrac{\lambda_0}{2}(1-C_{10}G(N_2^2))N_2 \\
&\quad -\tfrac{k_p}{2}(\mathcal{F}_{im}(N_2)\cos(\Delta\delta)-\mathcal{F}_{re}(N_2)\sin(\Delta\delta))) \\
&\quad -\lambda_{10}(-\tfrac{f_0}{2}\cos(\delta_2)-\tfrac{2\sigma+1}{2}(1-C_{10}G(N_2^2))N_2+\tfrac{\lambda_0\lambda_{10}}{2}N_2+\tfrac{N_2}{2} \\
&\quad +\tfrac{k_p}{2}(\mathcal{F}_{im}(N_2)\sin(\Delta\delta)+\mathcal{F}_{re}(N_2)\cos(\Delta\delta))) \\
g(N_2,\delta_2) &= \lambda_{10}(-\tfrac{f_0}{2}\sin(\delta_2)-\tfrac{(2\sigma+1)\lambda_{10}}{2}N_2-\tfrac{\lambda_0}{2}(1-C_{10}G(N_2^2))N_2 \\
&\quad -\tfrac{k_p}{2}(\mathcal{F}_{im}(N_2)\cos(\Delta\delta)-\mathcal{F}_{re}(N_2)\sin(\Delta\delta))) \\
&\quad (1-C_{10}G(N_2^2)-2C_{10}N_2^2G'(N_2^2))(-\tfrac{f_0}{2}\cos(\delta_2)-\tfrac{2\sigma+1}{2}(1-C_{10}G(N_2^2))N_2 \\
&\quad +\tfrac{\lambda_0\lambda_{10}}{2}N_2+\tfrac{N_2}{2}+\tfrac{k_p}{2}(\mathcal{F}_{im}(N_2)\sin(\Delta\delta)+\mathcal{F}_{re}(N_2)\cos(\Delta\delta)))
\end{aligned}
$$

REFERENCES

[1] A. F. Vakakis, Inducing passive nonlinear energy sinks in vibrating systems, *ASME Journal of Vibration and Acoustics*, **123**, 324–332, 2001.

[2] O. V. Gendelman, L. I. Manevitch, A. F. Vakakis, R. M'Closkey, Energy pumping in nonlinear mechanical oscillators I: dynamics of the underlying hamiltonian systems, *ASME Journal of Applied Mechanics*, **68**, 34–41, 2001.

[3] A. F. Vakakis, O. V. Gendelman, energy pumping in nonlinear mechanical oscillators II: resonance capture. *ASME Journal of Applied Mechanics*, **68**, 42–48, 2001.

[4] A. F. Vakakis, O. V. Gendelman, L. A. Bergman, D. M. McFarland, G. Kerschen, Y. S. Lee, *Nonlinear Trageted Energy Transfer in Mechanical and Structural Systems I*, Springer, 2009.

[5] A. F. Vakakis, O. V. Gendelman, L. A. Bergman, D. M. McFarland, G. Kerschen, Y. S. Lee, *Nonlinear Trageted Energy Transfer in Mechanical and Structural Systems II*, Springer, 2009.

[6] D. M. McFarland, G. Kerschen, J. J. Kowtko, Y. S. Lee, L. A. Bergman, A. F. Vakakis, Experimental investigation of targeted energy transfers in strongly and nonlinearly coupled oscillators, *The Journal of the Acoustical Society of America*, **118**, 791–799, 2005.

[7] G. Kerschen, J. J. Kowtko, D. M. McFarland, L. A. Bergman, A. F. Vakakis, Theoretical and experimental study of multimodal targeted energy transfer in a system of coupled oscillators. *Nonlinear Dynamics*, **47**, 285–309, 2007.

[8] G. Kerschen, J. J. Kowtko, D. M. McFarland, Y. S. Lee, L. A. Bergman, A. F. Vakakis, Experimental demonstration of transient resonance capture in a system of two coupled oscillators with essential stiffness nonlinearity. *Journal of Sound and Vibration*, **299**, 822–838, 2007.

[9] E. Gourdon, N. A. Alexander, C. A. Taylor, C.-H. Lamarque, S. Pernot, Nonlinear energy pumping under transient forcing with strongly nonlinear coupling: theoretical and experimental results. *Journal of Sound and Vibration*, **300**, 522–551, 2007.

[10] Y. S. Lee, G. Kerschen, D. M. McFarland, W. J. Hill, C. Nichkawde, T. W. Strganac, L. A. Bergman, A. F. Vakakis, Suppressing aeroelastic instability using broadband passive targeted energy transfers, part 2: experiments. *AIAA Journal*, **45**, 2391–2400, 2007.

[11] A. Ture Savadkoohi, B. Vaurigaud, C.-H. Lamarque, S. Pernot S., Targeted energy transfer with parallel nonlinear energy sinks, part II: theory and experiments, *Nonlinear dynamics*, **67** , 37–46, 2012.

[12] R. Bellet, B. Cochelin, R. Côte, P.-O. Mattei, Enhancing the dynamic range of targeted energy transfer in acoustics using several nonlinear membrane absorbers. *Journal of Sound and Vibration*, **331** , 5657–5668, 2012.

[13] F. Nucera, A. F. Vakakis, D. M. McFarland, L. A. Bergman, G. Kerschen, Targeted energy transfers in vibro-impact oscillators for seismic mitigation. *Nonlinear Dynamics*, **50**, 651–677, 2007.

[14] Y. S. Lee, F. Nucera, A. F. Vakakis, D. M. McFarland, L. A. Bergman, Periodic orbits, damped transitions and targeted energy transfers in oscillators with vibro-impact attachments. *Physica D*, **238**, 1868–1896, 2009.

[15] O. V. Gendelman, Analytic treatment of a system with a vibro-impact nonlinear energy sink *Journal of Sound and Vibration*, **331**, 4599–4608, 2012.

[16] O.V. Gendelman, Targeted energy transfer in systems with non-polynomial nonlinearity. *Journal of Sound and Vibration*, **315**, 732–745, 2008.

[17] C.-H. Lamarque, O.V. Gendelman, A. Ture Savadkoohi, E. Etcheverria, Targeted energy transfer in mechanical systems by means of non-smooth nonlinear energy sink. *Acta Mechanica*, **221**, 175–200, 2011.

[18] A. Ture Savadkoohi, C.-H. Lamarque, Z. Dimitrijevic, Vibratory energy exchange between a linear and a non-smooth system in the presence of the gravity, *Nonlinear Dynamics*, **70**, 1473–1483, 2012.

[19] F. Schmidt, C.-H. Lamarque, Energy Pumping for Mechanical Systems involving Non-Smooth Saint-Venant terms. *International Journal of Non-Linear Mechanics*, **45**, 866–875, 2010.

[20] J. Bastien, M. Schatzman, C.-H. Lamarque, Study of some rheological models with a finite number of degrees of freedom. *European Journal of Mechanics A/Solids*, **19**, 277–307, 2000.

[21] C.-H. Lamarque, F. Bernardin, J. Bastien, Study of a rheological model with a friction term and a cubic term: deterministic and stochastic cases, *European Journal of Mechanics, A/Solids*, **24**, 572–592, 2005.

[22] C.-H. Lamarque, A. Ture Savadkoohi, E. Etcheverria, Z. Dimitrijevic, Multi-scales dynamics of two coupled non-smooth systems. *International Journal of Bifurcation and Chaos*, **22**, 125029 1–18, 2012.

[23] L. I. Manevitch, The description of localized normal modes in a chain of nonlinear coupled oscillators using complex variables. *Nonlinear Dynamics*, **25**, 95–109, 2001.

[24] A. H. Nayfeh , D. T. Mook, *Nonlinear oscillations*, John Wiley and Sons, 1979.

[25] Y. Starosvetsky , O. V. Gendelman, Strongly modulated response in forced 2DOF oscillatory system with essential mass and potential asymmetry. *Physica D*, **237**: 1719–1733, 2008.